IEEE Access
Multidisciplinary ⋮ Rapid Review ⋮ Open Access Journal

Received 28 July 2022, accepted 5 August 2022, date of publication 16 August 2022, date of current version 19 August 2022.
Digital Object Identifier 10.1109/ACCESS.2022.3198698

THEORY

Barrier Robust Iterative Learning Control for Nonlinear Systems With Both Nonparametric Uncertainties and Time-Iteration-Varying Parametric Uncertainties Under Alignment Condition

ZHONGJIE HE, (Member, IEEE), AND JIANNING LI
School of Automation, Hangzhou Dianzi University, Hangzhou 310018, China
Corresponding author: Zhongjie He (zhongjiehezj@outlook.com)

This work was supported in part by the Zhejiang Provincial Natural Science Foundation of China under Grant LGG20F030003 and Grant 2021C01144.

ABSTRACT In this work, a barrier robust iterative learning control approach for a class of nonlinear systems with both nonparametric uncertainties and time-iteration-varying parametric uncertainties is studied. The nonparametric uncertainties meet Lipschitz-like continuous condition, and the time-iteration-varying parametric uncertainties are generated by a high-order internal model(HOIM). A barrier Lyapunov function is adopted for controller design to achieve system constraints. In light of the fact that the reference trajectory is smoothly closed, alignment condition is used to overcome the initial position problem of ILC. Robust learning method is used to compensate for the nonparametric uncertainties. According to the characteristic of HOIM, the time-iteration-varying parametric uncertainties is estimated by using difference learning method. Excellent tracking performance may be obtained as the iteration number increases, with the error quadratic form constrained during each iteration. Numerical Simulation results show the effectiveness of the propose barrier robust iterative learning control scheme.

INDEX TERMS Nonlinear systems, iterative learning control, high-order internal model, barrier Lyapunov function, alignment condition.

I. INTRODUCTION

Iterative learning control (ILC) is indeed a suitable control strategy for those nonlinear systems that operate repeatedly during a finite time interval. With the prominent ability in rejecting repetitive disturbances or uncertainties, even where system modeling is very difficult, ILC system is still promising to achieve good performance [1], [2], [3], [4], [5], [6]. Based on the invariance property, the iteration-independent parameter(s) in a closed-loop ILC system may be gradually estimated by using the information of system error, such that, as the iteration number increases, excellent tracking performance may be achieved over the whole time interval. The research on ILC algorithm originated in the early 80s of last century. Nowadays, ILC is widely applied in the controller design of robotic systems, batch reactor, traffic flow, motor driver, etc [7], [8], [9], [10].

There are some challenges in the research of ILC, three of which will be discussed in this work. The first problem is about the compensation strategy of uncertainties. Direct parameter-estimation method is suitable for dealing with those uncertainties whose structures are available but the parameters are unknown. However, this strategy is not practical to nonparametric uncertainties and with iteration-varying uncertainties. Robust method is a useful solution to compensate for nonparametric uncertainties,

The associate editor coordinating the review of this manuscript and approving it for publication was Jinquan Xu.

that is, a feedback term may be designed according to the upper bound of nonparametric uncertainty [11]. Another common solution is to approximate nonparametric uncertainties by using fuzzy systems or neural networks [29], [34]. The iteration-varying factors generated by high-order internal model (HOIM) has been a focus of ILC research in recent years. In [12], Yin *et al.* proposed a HOIM-based ILC scheme for continuous-time nonlinear systems with time-iteration-varying parameters. In [13], Yu *et al.* developed a HOIM-based adaptive ILC approach for a class of MIMO discrete-time nonlinear systems with time-iteration-varying unknown parameters. In [14], Wan and Li investigated the ILC algorithms for 2-D linear discrete FMMI systems to track the HOIM-based iteration-varying reference trajectories. Hitherto, there have been a few research reports focusing on adaptive ILC algorithms for systems with nonparametric uncertainties alone, or for systems with time-iteration-varying parametric uncertainties generated by HOIM alone. However, few results involve ILC algorithms for nonliner systems with both nonparametric uncertainties and time-iteration-varying parametric uncertainties generated by HOIM.

The second issue about ILC is the system constraint. Most practical systems are subject to certain constraints for physical limits or performance requirements, which has enticed sustained research interest from control community in the past decades. A lot of reports on state constraints, output constraints or tracking error constraints have been proposed [15], [16], [17], [18], [19], [20]. At present, in the context of adaptive ILC, barrier Lyaponov function approach is the mainstream technique for implementing system constraints. In [21], based on backstepping method, an output-constrained adaptive ILC is developed for nonlinear systems under alignment condition. In [22], an error-constraint ILC for MIMO systems under alignment condition is discussed. In [23], a state-constrained error-tracking ILC scheme is proposed for nonparametric uncertain systems with arbitrary initial error. In [24], a neural network based adaptive ILC scheme is proposed for nonlinear uncertain systems with state constraints. The spatial adaptive ILC with position constraint has been discussed in [25] and [26], respectively. In [27], the filtering error-like variable is constrained for nonlinear systems with parametric uncertainties generated by a HOIM.

The third issue about ILC concerns the initial condition of ILC systems [28]. In many ILC literatures, there exist a fundamental assumption that the initial system errors of ILC systems must be zero. To meet this assumption, perfect resetting or repositioning with zero initial error is necessary at the very beginning of each iteration cycle. Since this perfect resetting or repositioning can not be met in actual systems, this special assumption is really a stumbling block to apply ILC theory into practice. Through continuous exploration, several solutions have been proposed for relaxing this assumption in ILC system design [29], [30], [31], such as time-varying boundary layer technique, initial rectification approach, alignment condition, etc. Among these solutions, alignment condition is practical for uncertain ILC systems whose reference trajectories are smoothly closed in space [32], [33]. To date, how to develop an effective ILC algorithm for the nonzero initial error systems where there exist nonparametric uncertainties and iteration-varying uncertainties, and exist the requirement of system constraint, has not been addressed yet.

Motivated by the aforementioned studies, in this work, we present a barrier adaptive ILC scheme for a class of nonlinear systems with nonparametric uncertainties and time-iteration-varying parametric uncertainties under alignment condition, where the nonparametric nonlinearities satisfy local Lipschitz conditions and the time-iteration-varying parametric uncertainties are generated by a HOIM. To address this constraint requirement, we adopt a error quadratic form-based barrier Lyapunov function to controller design. Alignment condition is used to deal with the nonzero initial error of ILC systems.

Compared to the result of similar research, the main contributions are summarized as follows:

1) A robust adaptive iterative learning controller is developed for nonlinear systems with time-iteration-varying parametric uncertainties and nonparametric uncertainties generated by HOIM. The assumption on uncertainty structure in this work is lower than that in similar works.
2) To achieve system constraint during operation, an error quadratic form barrier Lyapunov function is constructed to design iterative learning controller for nonlinear systems with nonparametric uncertainties and iteration-time-varying parametric uncertainties generated by HOIM.
3) Adaptive ILC algorithms are developed for the case with iteration-independent time-varying input gain and for the case with state-dependent input gain, respectively.

The remainder of this paper is organized as follows. The system model and control objective are described in Section II. A barrier adaptive ILC scheme is developed in Section III. The proof on system convergence and system constraints is provided in Section IV. Section V presents the barrier robust ILC approach for systems with state-dependent input gain. In Section VI, numerical simulation results are provided to compare the proposed barrier adaptive ILC against the barrier-free adaptive ILC. Finally, Section VII concludes the work.

II. PROBLEM FORMULATION

Consider a class of nonlinear systems which repetitively operates during $t \in [0, T]$ as follows:

$$\begin{cases} \dot{x}_{i,k}(t) = x_{i+1,k}(t), \quad i = 1, 2, \cdots, n-1 \\ \dot{x}_{n,k}(t) = \boldsymbol{\vartheta}_k^T(t)\boldsymbol{\zeta}(\boldsymbol{x}_k(t)) + f(\boldsymbol{x}_k(t), t) + g(t)u_k(t), \end{cases} \tag{1}$$

where k is the iteration index, $\boldsymbol{x}_k(t) = [x_{1,k}(t), x_{2,k}(t), \cdots, x_{n,k}(t)]^T \in \mathbb{R}^n$, $g(t)$ is the unknown positive iteration-independent time-varying input gain, $u_k(t)$ is the control input, and $\boldsymbol{\zeta}(\boldsymbol{x}_k(t)) = [\zeta_1(\boldsymbol{x}_k(t)), \zeta_2(\boldsymbol{x}_k(t)), \cdots, \zeta_p(\boldsymbol{x}_k(t))]^T$

is a continuous basis function vector. The reference trajectory $\boldsymbol{x}_d(t)$ is smoothly closed,

$$\boldsymbol{x}_d(T) = \boldsymbol{x}_d(0). \tag{2}$$

and

Assumption 1: $f(\boldsymbol{x}_k(t), t)$ satisfies the Liphitz-like continuous condition as

$$|f(\boldsymbol{x}_k, t) - f(\boldsymbol{x}_d, t)| \leq \alpha(\boldsymbol{x}_k, \boldsymbol{x}_d, t)\|\boldsymbol{x}_k - \boldsymbol{x}_d\|, \tag{3}$$

where $\alpha(\boldsymbol{x}_k, \boldsymbol{x}_d, t)$ is a known continuous function [32].

Assumption 2: $\boldsymbol{\vartheta}_k = [\vartheta_{1,k}, \vartheta_{2,k}, \cdots, \vartheta_{p,k}]^T \in \mathbb{R}^p$. For $j = 1, 2, \cdots, p$, $\vartheta_{j,k}$ is an unknown bounded parameter with respect to both t and k as follows [12]:

$$\vartheta_{j,k}(t) = w_{j,1}\vartheta_{j,k-1}(t) + \cdots + w_{j,m_j}\vartheta_{j,k-m_j}(t), \tag{4}$$

where $w_{j,1}, \cdots, w_{j,m_j}$ are known constant coefficients. $\vartheta_{j,-1}(t), \cdots, \vartheta_{j,-m_j}(t)$ are unknown basis functions that are linearly independent.

In this work, we will develop adaptive iterative learning control scheme for system (1), and then extend it to the systems with state-dependent input gains (42). The control task is to make $\boldsymbol{x}_k(t)$ track its reference trajectory $\boldsymbol{x}_d(t)$ under $\boldsymbol{x}_k(0) \neq \boldsymbol{x}_d(0)$. For the purpose of brevity, the argument(s) of a function may be omitted while the context is sufficiently explicit.

Remark 1: In this work, the structure of $f(\boldsymbol{x}_k, t)$ in (1) is unknown. If the structure of $f(\boldsymbol{x}_k, t)$ is assumed to be known, then this function can be parameterizable as

$$f(\boldsymbol{x}_k, t) = \boldsymbol{w}^T(t)\boldsymbol{\xi}(\boldsymbol{x}_k). \tag{5}$$

Substituting (5) into (1) yields

$$\begin{cases} \dot{x}_{i,k} = x_{i+1,k}(t), \quad i = 1, 2, \cdots, n-1 \\ \dot{x}_{n,k} = \boldsymbol{\vartheta}_k^T(t)\boldsymbol{\zeta}(\boldsymbol{x}_k) + \boldsymbol{w}^T(t)\boldsymbol{\xi}(\boldsymbol{x}_k) + g(t)u_k, \end{cases} \tag{6}$$

which is actually the system model considered in literature [27]. Hence, this work studies the ILC design under lower uncertainty assumption condition than [27].

III. CONTROL SYSTEM DESIGN

By letting

$$\boldsymbol{\upsilon}_{j,k} = [\vartheta_{j,k-m_j+1}, \vartheta_{j,k-m_j}, \cdots, \vartheta_{j,k-1}, \vartheta_{j,k}]^T \tag{7}$$

and

$$W_j = \begin{pmatrix} 0 & 1 & 0 & \cdots & 0 \\ 0 & 0 & 1 & \cdots & 0 \\ \vdots & \vdots & \vdots & \ddots & \vdots \\ w_{j,m_j} & w_{j,m_j-1} & w_{j,m_j-2} & \cdots & w_{j,1} \end{pmatrix},$$

we can rewrite (4) as

$$\boldsymbol{\upsilon}_{j,k} = W_j^1\boldsymbol{\upsilon}_{j,k-1} = \cdots = W_j^k\boldsymbol{\upsilon}_{j,0}. \tag{8}$$

Let $\boldsymbol{\varphi}_{j,k}^T$ denote the last row of matrix W_j^k. From (7) and (8), we have

$$\vartheta_{j,k} = \boldsymbol{\upsilon}_{j,0}^T\boldsymbol{\varphi}_{j,k}. \tag{9}$$

To overcome the initial position problem of ILC, the initial state in the kth iteration is taken as

$$\boldsymbol{x}_k(0) = \boldsymbol{x}_{k-1}(T) \tag{10}$$

for $k = 1, 2, 3, \cdots$. This strategy is called alignment condition in the field of ILC [32].

Remark 2: In [27], the technique of time-varying boundary layer is used to deal with the initial position problem of ILC. In the cases that the reference trajectories are smoothly closed in space, both time-varying boundary layer technique and alignment condition are reasonable solution to initial position problem of ILC. Between them, the latter is easier to implement since the construction and use of time-varying boundary layer is a bit troublesome job.

Define $\boldsymbol{e}_k = [e_{1,k}, e_{2,k}, \cdots, e_{n,k}]^T = \boldsymbol{x}_k - \boldsymbol{x}_d$. On the basis of (2), (10) and (1), we can respectively get

$$\boldsymbol{e}_k(0) = \boldsymbol{e}_{k-1}(T) \tag{11}$$

and

$$\dot{\boldsymbol{e}}_k = A_c\boldsymbol{e}_k + \boldsymbol{b}[\boldsymbol{c}^T\boldsymbol{e}_k + \textstyle\sum_{j=1}^p(\boldsymbol{\upsilon}_{j,0}^T\boldsymbol{\varphi}_{j,k}\zeta_{j,k}) + f(\boldsymbol{x}_k, t) + gu_k - \dot{x}_{n,d}], \tag{12}$$

where $\boldsymbol{c} = [c_0, c_1, \cdots, c_{n-1}]^T$, $\boldsymbol{b} = [0, 0, \cdots, 0, 1]^T$,

$$A_c = \begin{pmatrix} 0 & 1 & 0 & \cdots & 0 \\ 0 & 0 & 1 & \cdots & 0 \\ \vdots & \vdots & \vdots & & \vdots \\ -c_0 & -c_1 & -c_2 & \cdots & -c_{n-1} \end{pmatrix}.$$

The parameter vector $\boldsymbol{c}$ is chosen properly to make $p(s) = s^n + c_{n-1}s^{n-1} + \cdots + c_2s^2 + c_1s + c_0$ be a Hurwitz polynomial. For such a matrix A_c, there must exist symmetric positive definite matrices P and Q satisfying $PA_c + A_c^TP = -Q$ and

$$\lambda_Q - 1 > 0, \tag{13}$$

where λ_Q is the minimum eigenvalue of Q.

Define a candidate barrier Lyappunov function

$$V_k(t) = \frac{\boldsymbol{e}_k^TP\boldsymbol{e}_k}{2(b_e - \boldsymbol{e}_k^TP\boldsymbol{e}_k)}, \tag{14}$$

where the constraint parameter b_e satisfies $b_e > \boldsymbol{e}_0^T(0)P\boldsymbol{e}_0(0)$. Taking the time derivative of V_k, we obtain the following expression:

$$\begin{aligned} \dot{V}_k &= \frac{\sigma_k}{2}(\dot{\boldsymbol{e}}_k^TP\boldsymbol{e}_k + \boldsymbol{e}_k^TP\dot{\boldsymbol{e}}_k) \\ &= -\frac{\sigma_k}{2}\boldsymbol{e}_k^TQ\boldsymbol{e}_k + \sigma_k\boldsymbol{e}_k^TP\boldsymbol{b}g[g^{-1}\boldsymbol{c}^T\boldsymbol{e}_k + g^{-1}\sum_{j=1}^p(\boldsymbol{\upsilon}_{j,0}^T\boldsymbol{\varphi}_{j,k} \\ &\quad \cdot\zeta_{j,k}) + g^{-1}f(\boldsymbol{x}_k, t) + u_k - g^{-1}\dot{x}_{n,d}], \end{aligned} \tag{15}$$

where $\sigma_k = \frac{b_e}{(b_e - \boldsymbol{e}_k^TP\boldsymbol{e}_k)^2}$. On the basis of (3), we have

$$\begin{aligned} &\sigma_k\boldsymbol{e}_k^TP\boldsymbol{b}f(\boldsymbol{x}_k, t) - \sigma_k\boldsymbol{e}_k^TP\boldsymbol{b}f(\boldsymbol{x}_d) \\ &\quad \leq \sigma_k|\boldsymbol{e}_k^TP\boldsymbol{b}|\alpha(\boldsymbol{x}_k, \boldsymbol{x}_d)\|\boldsymbol{e}_k\| \\ &\quad \leq \frac{\sigma_k}{2}\|\boldsymbol{e}_k\|^2 + \frac{\sigma_k}{2}\alpha^2(\boldsymbol{x}, \boldsymbol{x}_d)(\boldsymbol{e}_k^TP\boldsymbol{b})^2. \end{aligned} \tag{16}$$

From (15) and (16), we get

$$\begin{aligned}\dot{V}_k \le & -\frac{\sigma_k}{2}\boldsymbol{e}_k^T Q \boldsymbol{e}_k + \sigma_k \boldsymbol{e}_k^T P\boldsymbol{b} g[g^{-1}\boldsymbol{c}^T\boldsymbol{e}_k + u_k - g^{-1}\dot{x}_{n,d} \\ & + g^{-1}\sum_{j=1}^{p}(\boldsymbol{\upsilon}_{j,0}^T\boldsymbol{\varphi}_{j,k}\zeta_{j,k}) + g^{-1}f(\boldsymbol{x}_d)] \\ & + \frac{\sigma_k}{2}\|\boldsymbol{e}_k\|^2 + \frac{\sigma_k}{2}\alpha^2(\boldsymbol{x},\boldsymbol{x}_d)(\boldsymbol{e}_k^T P\boldsymbol{b})^2. \qquad (17)\end{aligned}$$

Define $\boldsymbol{\varpi} = [g^{-1}, g^{-1}f(\boldsymbol{x}_d) - g^{-1}\dot{x}_{n,d}, (2g)^{-1}]^T$, $\boldsymbol{\psi}_k = [\boldsymbol{c}^T\boldsymbol{e}_k, 1, \alpha^2(\boldsymbol{x},\boldsymbol{x}_d)\boldsymbol{e}_k^T P\boldsymbol{b}]^T$ and $\boldsymbol{z}_j = g^{-1}\boldsymbol{\upsilon}_{j,0}$. Then, (17) can be rewritten as

$$\dot{V}_k(t) \le \sigma_k \boldsymbol{e}_k^T P\boldsymbol{b} g\big[\boldsymbol{\varpi}^T\boldsymbol{\psi}_k + \sum_{j=1}^{p}(\boldsymbol{z}_j^T\boldsymbol{\varphi}_{j,k}\zeta_{j,k}) + u_k\big] - \frac{\sigma_k}{2}(\lambda_Q - 1)\|\boldsymbol{e}_k\|^2. \qquad (18)$$

where λ_Q is the minimum eigenvalue of matrix Q.

On the basis of (18), we design the control law and learning laws as follows:

$$u_k = -\mu_1\boldsymbol{e}_k^T P\boldsymbol{b} - \boldsymbol{\varpi}_k^T\boldsymbol{\psi}_k - \sum_{j=1}^{p}(\boldsymbol{z}_{j,k}^T\boldsymbol{\varphi}_{j,k}\zeta_{j,k}), \qquad (19)$$

$$\boldsymbol{\varpi_k} = \mathrm{sat}_{\underline{\varpi},\bar{\varpi}}(\boldsymbol{\varpi}_{k-1}) + \mu_2\sigma_k\boldsymbol{e}_k^T P\boldsymbol{b}\boldsymbol{\psi}_k, \boldsymbol{\varpi}_{-1} = 0, \qquad (20)$$

$$\boldsymbol{z}_{j,k} = \mathrm{sat}_{\underline{z}_j,\bar{z}_j}(\boldsymbol{z}_{j,k-1}) + \mu_3\sigma_k\boldsymbol{e}_k^T P\boldsymbol{b}\boldsymbol{\varphi}_{j,k}\zeta_{j,k}, \boldsymbol{z}_{j,-1} = 0, \qquad (21)$$

where $\mu_1 > 0$, $\mu_2 > 0$ and $\mu_3 > 0$. The saturation function $\mathrm{sat}_{\cdot,\cdot}(\cdot)$ is defined as follows: For $\hat{\chi} \in \mathbb{R}$ used to estimate a scalar χ,

$$\mathrm{sat}_{\underline{\chi},\bar{\chi}}(\hat{\chi}) := \begin{cases} \bar{\chi}, & \text{if } \hat{a} > \bar{\chi} \\ \hat{\chi}, & \text{if } \underline{\chi} \le \hat{\chi} \le \bar{\chi} \\ \underline{\chi}, & \text{if } \hat{\chi} < \underline{\chi} \end{cases},$$

where $\underline{\chi}$ and $\bar{\chi}$ are the lower bound and upper bound of the scalar a, respectively; for a vector $\hat{\boldsymbol{\chi}} = [\hat{\chi}_1, \hat{\chi}_2, \cdots, \hat{\chi}_m] \in \mathbb{R}^m$, $\mathrm{sat}_{\underline{\chi},\bar{\chi}}(\hat{\boldsymbol{\chi}}) := \big[\mathrm{sat}_{\underline{\chi},\bar{\chi}}(\hat{\chi}_1), \mathrm{sat}_{\underline{\chi},\bar{\chi}}(\hat{\chi}_2), \cdots, \mathrm{sat}_{\underline{\chi},\bar{\chi}}(\hat{\chi}_m)\big]^T$. Fig. 1 is the block diagram of the proposed robust adaptive ILC system.

Remark 3: In (14), the error quadratic form is constrained during each iteration. In literature [27], the filtering error is constrained during each iteration. Thereby, the constraint strategy is different from each other.

IV. CONVERGENCE ANALYSIS

Theorem 1: Consider the nonlinear system (1) satisfying Assumption 1, Assumption 2, (2) and (10). The proposed robust iterative learning controller (19)-(21) guarantees the tracking performance and system stability as follows:

t1) $\boldsymbol{e}_k^T(t)P\boldsymbol{e}_k(t) < b_e$ holds during each iteration;

t2) All adjustable control parameters and internal signals are bounded;

t3) $\boldsymbol{e}_k(t) = 0$ may be achieved as the iteration number increases.

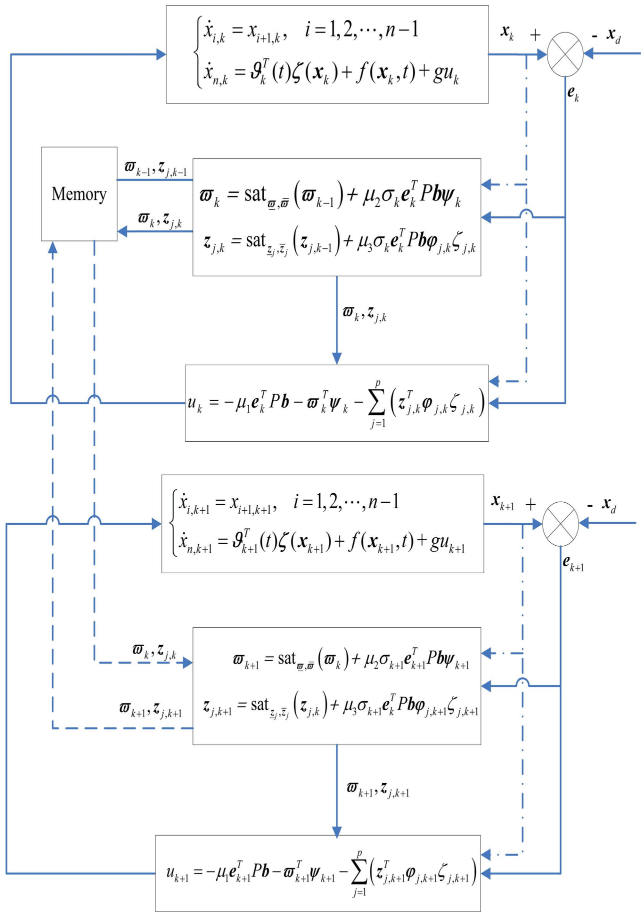

FIGURE 1. Block diagram of the robust adaptive ILC system.

Proof: t1) Let $\ell_Q = \lambda_Q - 1$. From (13), we can see that ℓ_Q is a positive number. Substituting (19) into (18) leads to

$$\dot{V}_k \le -\frac{\sigma_k}{2}\ell_Q\|\boldsymbol{e}_k\|^2 + \sigma_k\boldsymbol{e}_k^T P\boldsymbol{b} g\big[\tilde{\boldsymbol{\varpi}}_k^T\boldsymbol{\psi}_k + \sum_{j=1}^{p}(\tilde{\boldsymbol{z}}_{j,k}^T\boldsymbol{\varphi}_{j,k}\zeta_{j,k})\big], \qquad (22)$$

where $\tilde{\boldsymbol{\varpi}}_k = \boldsymbol{\varpi} - \boldsymbol{\varpi}_k$ and $\tilde{\boldsymbol{z}}_{j,k} = \boldsymbol{z}_j - \boldsymbol{z}_{j,k}$. Define a barrier Lyapunov functional as follows:

$$L_k = V_k + \frac{1}{2\mu_2}\int_0^t g\tilde{\boldsymbol{\varpi}}_k^T\tilde{\boldsymbol{\varpi}}_k d\tau + \sum_{j=1}^{p}\frac{1}{2\mu_3}\int_0^t g\tilde{\boldsymbol{z}}_{j,k}^T\tilde{\boldsymbol{z}}_{j,k}d\tau, \qquad (23)$$

From (22) and (23), we have

$$\begin{aligned}\dot{L}_k &= \dot{V}_k + \frac{g}{2\mu_2}\tilde{\boldsymbol{\varpi}}_k^T\tilde{\boldsymbol{\varpi}}_k + \frac{g}{2\mu_3}\sum_{j=1}^{p}\tilde{\boldsymbol{z}}_{j,k}^T\tilde{\boldsymbol{z}}_{j,k} \\ &\le -\frac{\sigma_k}{2}\ell_Q\|\boldsymbol{e}_k\|^2 + \sigma_k\boldsymbol{e}_k^T P\boldsymbol{b} g\big[\tilde{\boldsymbol{\varpi}}_k^T\boldsymbol{\psi}_k + \sum_{j=1}^{p}(\tilde{\boldsymbol{z}}_{j,k}^T\boldsymbol{\varphi}_{j,k}\zeta_{j,k})\big]\end{aligned}$$

$$+\frac{g}{2\mu_2}\tilde{\boldsymbol{\varpi}}_k^T\tilde{\boldsymbol{\varpi}}_k+\frac{g}{2\mu_3}\sum_{j=1}^{p}\tilde{z}_{j,k}^T\tilde{z}_{j,k}. \quad (24)$$

By using (20), we have

$$\begin{aligned}
&\sigma_k\boldsymbol{e}_k^T\boldsymbol{P}\boldsymbol{b}g\tilde{\boldsymbol{\varpi}}_k^T\boldsymbol{\psi}_k+\frac{g}{2\mu_2}\tilde{\boldsymbol{\varpi}}_k^T\tilde{\boldsymbol{\varpi}}_k\\
&=\frac{g}{2\mu_2}[-\boldsymbol{\varpi}_k^T\boldsymbol{\varpi}_k+\boldsymbol{\varpi}^T\boldsymbol{\varpi}-2\boldsymbol{\varpi}^T\text{sat}_{\underline{\varpi},\bar{\varpi}}(\boldsymbol{\varpi}_{k-1})\\
&\quad+2\boldsymbol{\varpi}_k^T\text{sat}_{\underline{\varpi},\bar{\varpi}}(\boldsymbol{\varpi}_{k-1})]\\
&=-\frac{g}{2\mu_2}[\boldsymbol{\varpi}_k-\text{sat}_{\underline{\varpi},\bar{\varpi}}(\boldsymbol{\varpi}_{k-1})]^T[\boldsymbol{\varpi}_k-\text{sat}_{\underline{\varpi},\bar{\varpi}}(\boldsymbol{\varpi}_{k-1})]\\
&\quad+\frac{g}{2\mu_2}[\text{sat}_{\underline{\varpi},\bar{\varpi}}(\boldsymbol{\varpi}_{k-1}^T)\text{sat}_{\underline{\varpi},\bar{\varpi}}(\boldsymbol{\varpi}_{k-1})+\boldsymbol{\varpi}^T\boldsymbol{\varpi}\\
&\quad-2\boldsymbol{\varpi}^T\text{sat}_{\underline{\varpi},\bar{\varpi}}(\boldsymbol{\varpi}_{k-1})]\\
&\le\frac{g}{2\mu_2}\text{sat}_{\underline{\varpi},\bar{\varpi}}(\boldsymbol{\varpi}_{k-1}^T)\text{sat}_{\underline{\varpi},\bar{\varpi}}(\boldsymbol{\varpi}_{k-1})+\frac{g}{2\mu_2}\boldsymbol{\varpi}^T\boldsymbol{\varpi}\\
&\quad-\frac{g}{\mu_2}\boldsymbol{\varpi}^T\text{sat}_{\underline{\varpi},\bar{\varpi}}(\boldsymbol{\varpi}_{k-1})].
\end{aligned} \quad (25)$$

Obviously, each term in the right side of inequality (25) is bounded. Therefore, there exits a positive number c_{ϖ}, which satisfies

$$\sigma_k\boldsymbol{e}_k^T\boldsymbol{P}\boldsymbol{b}g\tilde{\boldsymbol{\varpi}}_k^T\boldsymbol{\psi}_k+\frac{g}{2\mu_3}\tilde{\boldsymbol{\varpi}}_k^T\tilde{\boldsymbol{\varpi}}_k\le c_{\varpi}. \quad (26)$$

Similarly, by using (21), there exist a positive number $c_{z,j}$, which meets

$$\begin{aligned}
&\sigma_k\boldsymbol{e}_k^T\boldsymbol{P}\boldsymbol{b}g\tilde{z}_{j,k}^T\boldsymbol{\varphi}_{j,k}\zeta_{j,k}+\frac{g}{2\mu_3}\tilde{z}_{j,k}^T\tilde{z}_{j,k}\\
&=\frac{g}{2\mu_3}[-z_{j,k}^Tz_{j,k}+z_j^Tz_j-2z_j^T\text{sat}_{\underline{z}_j,\bar{z}_j}(z_{j,k-1})\\
&\quad+2z_{j,k}^T\text{sat}_{\underline{z}_j,\bar{z}_j}(z_{j,k-1})]\\
&=-\frac{g}{2\mu_3}[z_{j,k}-\text{sat}_{\underline{z}_j,\bar{z}_j}(z_{j,k-1})]^T[z_{j,k}-\text{sat}_{\underline{z}_j,\bar{z}_j}(z_{j,k-1})]\\
&\quad+\frac{g}{2\mu_3}[\text{sat}_{\underline{z}_j,\bar{z}_j}(z_{j,k-1}^T)\text{sat}_{\underline{z}_j,\bar{z}_j}(z_{j,k-1})+z_j^Tz_j\\
&\quad-2z_j^T\text{sat}_{\underline{z}_j,\bar{z}_j}(z_{j,k-1})]\\
&\le\frac{g}{2\mu_3}[\text{sat}_{\underline{z}_j,\bar{z}_j}(z_{j,k-1}^T)\text{sat}_{\underline{z}_j,\bar{z}_j}(z_{j,k-1})+z_j^Tz_j\\
&\quad-2z_j^T\text{sat}_{\underline{z}_j,\bar{z}_j}(z_{j,k-1})]\\
&\le c_{z,j}
\end{aligned} \quad (27)$$

From (26) and (27)

$$\dot{L}_k\le-\tfrac{\sigma_k}{2}\ell_Q\|\boldsymbol{e}_k\|^2+c_{\varpi}+\textstyle\sum_{j=1}^{p}c_{z,j} \quad (28)$$

Due to $\dot{L}_k\ge\dot{V}_k$, from (28), we have

$$\dot{V}_k\le-\tfrac{\ell_Qb_e}{2(b_e-\boldsymbol{e}_k^T\boldsymbol{P}\boldsymbol{e}_k)^2}\|\boldsymbol{e}_k\|^2+c_{\varpi}+\textstyle\sum_{j=1}^{p}c_{z,j} \quad (29)$$

Note that $\boldsymbol{e}_0^T(0)\boldsymbol{P}\boldsymbol{e}_0(0)<b_e$ holds. As shown in (29), if $\boldsymbol{e}_0^T(t)\boldsymbol{P}\boldsymbol{e}_0(t)$ increases to b_{e-} for any $t\in(0,T)$, then

$$\dot{V}_0(t)<0 \quad (30)$$

must happen. This means $V_0(t)$ must decrease before $\boldsymbol{e}_0^T(t)\boldsymbol{P}\boldsymbol{e}_0(t)$ increases to b_{e-} for $t\in(0,T)$. Due to $\boldsymbol{e}_0^T(0)\boldsymbol{P}\boldsymbol{e}_0(0)<b_e$, according to the definition of $V_k(t)$, we have

$$V_0(t)=\frac{1}{2(\frac{b_e}{\boldsymbol{e}_0^T(t)\boldsymbol{P}\boldsymbol{e}_0(t)}-1)}. \quad (31)$$

As shown in (31), the decease of $V_0(t)$ is equivalent to the decrease of $\boldsymbol{e}_0^T(t)\boldsymbol{P}\boldsymbol{e}_0(t)$. Thus, $\boldsymbol{e}_0^T(t)\boldsymbol{P}\boldsymbol{e}_0(t)<b_e$ is guaranteed for $t\in[0,T]$.

It follows from $\boldsymbol{e}_1(0)=\boldsymbol{e}_0(T)$ and $\boldsymbol{e}_0^T(t)\boldsymbol{P}\boldsymbol{e}_0(t)<b_e$ that $\boldsymbol{e}_1^T(0)\boldsymbol{P}\boldsymbol{e}_1(0)<b_e$ holds. Applying the similar deduction as above, we can conclude that $\boldsymbol{e}_1^T(t)\boldsymbol{P}\boldsymbol{e}_1(t)<b_e$ is guaranteed for $t\in[0,T]$. Further, we can prove that $\boldsymbol{e}_j^T(t)\boldsymbol{P}\boldsymbol{e}_j(t)<b_s$ is guaranteed for $t\in[0,T]$ when $j=2,3,\cdots$. This proves t1) of Theorem 1.

t2) According to $\boldsymbol{e}_k^T\boldsymbol{P}\boldsymbol{e}_k<b_e$, we can deduce that $\boldsymbol{e}_k$, $\boldsymbol{x}_k$, $\boldsymbol{\psi}_k$ and $\zeta_{j,k}$ are bounded. By the property of saturation function, we can obtain the boundedness of $\boldsymbol{\varpi_k}$ and $z_{j,k}$ from (20) and (21), respectively. Since each term on the right-hand side of (19) is bounded, u_k may be verified to be bounded. By using these above conclusions, we can see that $\dot{\boldsymbol{x}}_k$ and $\dot{\boldsymbol{e}}_k$ are from (1) and (12), respectively. This proves t2) of Theorem 1.

t3)

From (22), we have

$$V_k\le V_k(0)-\int_0^t\frac{\sigma_k}{2}\ell_Q\|\boldsymbol{e}_k\|^2d\tau+\int_0^t\sigma_k\boldsymbol{e}_k^T\boldsymbol{P}\boldsymbol{b}g\big[\tilde{\boldsymbol{\varpi}}_k^T\boldsymbol{\psi}_k+\sum_{j=1}^{p}(\tilde{z}_{j,k}^T\boldsymbol{\varphi}_{j,k}\zeta_{j,k})\big]d\tau. \quad (32)$$

While $k>0$, it is obvious that

$$\begin{aligned}
&L_k-L_{k-1}\\
&=V_k-V_{k-1}+\frac{1}{2\mu_2}\int_0^tg(\tilde{\boldsymbol{\varpi}}_k^T\tilde{\boldsymbol{\varpi}}_k-\tilde{\boldsymbol{\varpi}}_{k-1}^T\tilde{\boldsymbol{\varpi}}_{k-1})d\tau\\
&\quad+\sum_{j=1}^{p}\frac{1}{2\mu_3}\int_0^tg(\tilde{z}_{j,k}^T\tilde{z}_{j,k}-\tilde{z}_{j,k-1}^T\tilde{z}_{j,k-1})d\tau\\
&\le-\int_0^t\frac{\sigma_k}{2}\ell_Q\|\boldsymbol{e}_k\|^2d\tau+\int_0^t\sigma_k\boldsymbol{e}_k^T\boldsymbol{P}\boldsymbol{b}g\big[\tilde{\boldsymbol{\varpi}}_k^T\boldsymbol{\psi}_k\\
&\quad+\sum_{j=1}^{p}(\tilde{z}_{j,k}^T\boldsymbol{\varphi}_{j,k}\zeta_{j,k})\big]d\tau+V_k(0)-V_{k-1}\\
&\quad+\frac{1}{2\mu_2}\int_0^tg(\tilde{\boldsymbol{\varpi}}_k^T\tilde{\boldsymbol{\varpi}}_k-\tilde{\boldsymbol{\varpi}}_{k-1}^T\tilde{\boldsymbol{\varpi}}_{k-1})d\tau\\
&\quad+\sum_{j=1}^{p}\frac{1}{2\mu_3}\int_0^tg(\tilde{z}_{j,k}^T\tilde{z}_{j,k}-\tilde{z}_{j,k-1}^T\tilde{z}_{j,k-1})d\tau
\end{aligned} \quad (33)$$

Due to $(\boldsymbol{\varpi}-\boldsymbol{\varpi}_{k-1})^T(\boldsymbol{\varpi}-\boldsymbol{\varpi}_{k-1})\ge(\boldsymbol{\varpi}-\text{sat}_{\underline{\varpi},\bar{\varpi}}(\boldsymbol{\varpi}_{k-1}))^T(\boldsymbol{\varpi}-\text{sat}_{\underline{\varpi},\bar{\varpi}}(\boldsymbol{\varpi}_{k-1}))$, from (20), we have

$$\begin{aligned}
&\frac{g}{2\mu_2}(\tilde{\boldsymbol{\varpi}}_k^T\tilde{\boldsymbol{\varpi}}_k-\tilde{\boldsymbol{\varpi}}_{k-1}^T\tilde{\boldsymbol{\varpi}}_{k-1})+\sigma_k\boldsymbol{e}_k^T\boldsymbol{P}\boldsymbol{b}g\tilde{\boldsymbol{\varpi}}_k^T\boldsymbol{\psi}_k\\
&\le\frac{g}{2\mu_2}[(\boldsymbol{\varpi}-\boldsymbol{\varpi}_k)^T(\boldsymbol{\varpi}-\boldsymbol{\varpi}_k)-(\boldsymbol{\varpi}-\text{sat}_{\underline{\varpi},\bar{\varpi}}(\boldsymbol{\varpi}_{k-1}))^T\\
&\quad(\boldsymbol{\varpi}-\text{sat}_{\underline{\varpi},\bar{\varpi}}(\boldsymbol{\varpi}_{k-1}))]+\sigma_k\boldsymbol{e}_k^T\boldsymbol{P}\boldsymbol{b}g\tilde{\boldsymbol{\varpi}}_k^T\boldsymbol{\psi}_k
\end{aligned}$$

$$\leq \frac{g}{2\mu_2}(2\boldsymbol{\varpi} - \boldsymbol{\varpi}_k - \mathrm{sat}_{\underline{\varpi},\bar{\varpi}}(\boldsymbol{\varpi}_{k-1}))^T(\mathrm{sat}_{\underline{\varpi},\bar{\varpi}}(\boldsymbol{\varpi}_{k-1}) - \boldsymbol{\varpi}_k) + \sigma_k \boldsymbol{e}_k^T \boldsymbol{Pb} g \tilde{\boldsymbol{\varpi}}_k^T \boldsymbol{\psi}_k$$
$$\leq \frac{g}{\mu_2}(\boldsymbol{\varpi} - \boldsymbol{\varpi}_k)^T\left[\mathrm{sat}_{\underline{\varpi},\bar{\varpi}}(\boldsymbol{\varpi}_{k-1}) - \boldsymbol{\varpi}_k + \mu_2 \sigma_k \boldsymbol{e}_k^T \boldsymbol{Pb}\boldsymbol{\psi}_k\right]$$
$$= 0. \tag{34}$$

Applying $(z_j - z_{j,k-1})^T(z_j - z_{j,k-1}) \geq (z_j - \mathrm{sat}_{\underline{z},\bar{z}}(z_{j,k-1}))^T(z_j - \mathrm{sat}_{\underline{z},\bar{z}}(z_{j,k-1}))$, from (21), we have

$$\frac{g}{2\mu_3}(\tilde{z}_{j,k}^T\tilde{z}_{j,k} - \tilde{z}_{j,k-1}^T\tilde{z}_{j,k-1}) + \sigma_k \boldsymbol{e}_k^T \boldsymbol{Pb} g \tilde{z}_{j,k}^T \boldsymbol{\zeta}_{j,k}$$
$$\leq \frac{g}{2\mu_3}[(z_j - z_{j,k})^T(z_j - z_{j,k}) - (z_j - \mathrm{sat}_{\underline{z},\bar{z}}(z_{j,k-1}))^T(z_j - \mathrm{sat}_{\underline{z},\bar{z}}(z_{j,k-1}))] + \sigma_k \boldsymbol{e}_k^T \boldsymbol{Pb} g \tilde{z}_k^T \boldsymbol{\zeta}_{j,k}$$
$$\leq \frac{g}{2\mu_3}(2z_j - z_{j,k} - \mathrm{sat}_{\underline{z},\bar{z}}(z_{j,k-1}))^T(\mathrm{sat}_{\underline{z},\bar{z}}(z_{j,k-1}) - z_{j,k}) + \sigma_k \boldsymbol{e}_k^T \boldsymbol{Pb} g \tilde{z}_k^T \boldsymbol{\zeta}_k$$
$$\leq \frac{g}{\mu_3}(z_j - z_{j,k})^T\left[\mathrm{sat}_{\underline{z},\bar{z}}(z_{j,k-1}) - z_{j,k} + \mu_3 \sigma_k \boldsymbol{e}_k^T \boldsymbol{Pb}\boldsymbol{\zeta}_{j,k}\right]$$
$$= 0. \tag{35}$$

Substituting (34) and (35) into (33) yields

$$L_k - L_{k-1} \leq -\int_0^t \frac{\sigma_k}{2g}\ell_Q \|\boldsymbol{e}_k\|^2 d\tau + V_k(0) - V_{k-1}$$

and

$$L_k(T) - L_{k-1}(T) \leq -\int_0^T \frac{\sigma_k}{2}\ell_Q \|\boldsymbol{e}_k(\tau)\|^2 d\tau + V_k(0) - V_{k-1}(T). \tag{36}$$

From (11), we have

$$V_k(0) = V_{k-1}(T). \tag{37}$$

Combining (36) with (37) yields

$$L_k(T) - L_{k-1}(T) \leq -\int_0^T \frac{\sigma_k}{2}\ell_Q \|\boldsymbol{e}_k(\tau)\|^2 d\tau \leq -\frac{\ell_Q}{2b_e}\int_0^T \|\boldsymbol{e}_k(\tau)\|^2 d\tau. \tag{38}$$

Further, we have

$$L_k(T) \leq L_0(T) - \frac{\ell_Q}{2b_e}\sum_{i=1}^{k}\int_0^T \|\boldsymbol{e}_k(\tau)\|^2 d\tau. \tag{39}$$

By using the boundedness of $L_0(T)$ and the nonnegativity of $L_k(T)$, we have

$$\lim_{k\to+\infty}\int_0^T \|\boldsymbol{e}_k(\tau)\| d\tau = 0. \tag{40}$$

Taking advantage of the conclusion in t2), we can see that $\dot{\boldsymbol{e}}_k$ is bounded and $\boldsymbol{e}_k$ is equicontinuous. Hence, it follows from (40) that

$$\lim_{k\to+\infty}\boldsymbol{e}_k(t) = 0. \tag{41}$$

This proves t3) of Theorem 1. ■

In this work, difference learning method is used to design adaptive learning laws. Through achieving $\boldsymbol{e}_k^T(t)\boldsymbol{P}\boldsymbol{e}_k(t) < b_e$ during each iteration, the maximum of $\|\boldsymbol{e}_k\|$ is constrained in a preseted range.

V. BARRIER ROBUST ILC EXTENSION TO PLANTS WITH STATE-DEPENDENT INPUT GAINS

The input gain $g(t)$ in system (1) is time-varying but iteration-independent. In the section, we consider a class of more general uncertain systems as follows:

$$\begin{cases} \dot{x}_{i,k} = x_{i+1,k}, \quad i = 1, 2, \cdots, n-1 \\ \dot{x}_{n,k} = \boldsymbol{\vartheta}_k^T(t)\boldsymbol{\zeta}(\boldsymbol{x}_k) + f(\boldsymbol{x}_k, t) + g(\boldsymbol{x}_k, t)u_k, \end{cases} \tag{42}$$

where $g(\boldsymbol{x}_k, t)$ is a state-dependent function.

Assumption 3: There exist known functions $g_m(\boldsymbol{x}_k, t) > 0$ and $\beta(\boldsymbol{x}_k, \boldsymbol{x}_d, t) \geq 0$ [32], satisfying $g(\boldsymbol{x}_k, t) \geq g_m(\boldsymbol{x}_k, t)$ and

$$|g(\boldsymbol{x}_k, t) - g(\boldsymbol{x}_d, t)| \leq \beta(\boldsymbol{x}_k, \boldsymbol{x}_d, t)\|\boldsymbol{x}_k - \boldsymbol{x}_d\|. \tag{43}$$

For brevity, let g_k and g_d denote $g(\boldsymbol{x}_k, t)$ and $g(\boldsymbol{x}_d, t)$, respectively. Similar to (15), by taking the time derivative of $V_k(t) = \frac{\boldsymbol{e}_k^T\boldsymbol{P}\boldsymbol{e}_k}{2(b_e - \boldsymbol{e}_k^T\boldsymbol{P}\boldsymbol{e}_k)}$, we have

$$\dot{V}_k \leq -\frac{\sigma_k}{2}\boldsymbol{e}_k^T\boldsymbol{Q}\boldsymbol{e}_k + \sigma_k\boldsymbol{e}_k^T\boldsymbol{Pb}[\boldsymbol{c}^T\boldsymbol{e}_k + g_k u_k - \dot{x}_{n,d} + \sum_{j=1}^{p}(\boldsymbol{\upsilon}_{j,0}^T\boldsymbol{\varphi}_{j,k}\zeta_{j,k}) + f(\boldsymbol{x}_k, t)]. \tag{44}$$

According to (3), we get

$$\boldsymbol{e}_k^T\boldsymbol{Pb}[f(\boldsymbol{x}_k, t) - f(\boldsymbol{x}_d, t)] \leq |\boldsymbol{e}_k^T\boldsymbol{Pb}|\alpha(\boldsymbol{x}, \boldsymbol{x}_d, t)\|\boldsymbol{e}_k\| \leq \frac{1}{4}\|\boldsymbol{e}_k\|^2 + \alpha^2(\boldsymbol{x}, \boldsymbol{x}_d, t)(\boldsymbol{e}_k^T\boldsymbol{Pb})^2. \tag{45}$$

By using (43), we obtain

$$\boldsymbol{e}_k^T\boldsymbol{Pb}g_k u_k = \boldsymbol{e}_k^T\boldsymbol{Pb}(g_k u_k - g_k u_{dk} + g_k u_{dk} - g_d u_{dk} + g_d u_{dk})$$
$$\leq \boldsymbol{e}_k^T\boldsymbol{Pb}(g_k u_k - g_k u_{dk} + g_d u_{dk}) + |\boldsymbol{e}_k^T\boldsymbol{Pb}||u_{dk}|\alpha_{gk}\|\boldsymbol{e}_k\|$$
$$\leq \boldsymbol{e}_k^T\boldsymbol{Pb}(g_k u_k - g_k u_{dk} + g_d u_{dk}) + \frac{1}{4}\|\boldsymbol{e}_k\|^2 + \beta^2(\boldsymbol{x}, \boldsymbol{x}_d, t)u_{dk}^2(\boldsymbol{e}_k^T\boldsymbol{Pb})^2. \tag{46}$$

Then, substituting (45) and (46) into (44), we have

$$\dot{V}_k \leq -\frac{\sigma_k}{2}\boldsymbol{e}_k^T\boldsymbol{Q}\boldsymbol{e}_k + \sigma_k\boldsymbol{e}_k^T\boldsymbol{Pb}(g_k u_k - g_k u_{dk}) + \sigma_k\boldsymbol{e}_k^T\boldsymbol{Pb}g_d[u_{dk} + g_d^{-1}\boldsymbol{c}^T\boldsymbol{e}_k - g_d^{-1}\dot{x}_{n,d} + g_d^{-1}\sum_{j=1}^{p}(\boldsymbol{\upsilon}_{j,0}^T\boldsymbol{\varphi}_{j,k}\zeta_{j,k}) + g_d^{-1}f(\boldsymbol{x}_d, t)]$$
$$+\frac{\sigma_k}{2}\|\boldsymbol{e}_k\|^2 + \sigma_k\alpha^2(\boldsymbol{x}, \boldsymbol{x}_d, k)(\boldsymbol{e}_k^T\boldsymbol{Pb})^2 + \sigma_k\beta^2(\boldsymbol{x}_k, \boldsymbol{x}_d, t)u_{dk}^2(\boldsymbol{e}_k^T\boldsymbol{Pb})^2. \tag{47}$$

Define $\boldsymbol{\eta} = [g_d^{-1}, g_d^{-1}f(\boldsymbol{x}_d, t) - g_d^{-1}\dot{x}_{n,d}]^T$, $\boldsymbol{\chi}_k = [\boldsymbol{c}^T\boldsymbol{e}_k, 1]^T$ and $\boldsymbol{\omega}_j = g_d^{-1}\boldsymbol{\upsilon}_{j,0}$. Then, (48) can be rewritten as

$$\begin{aligned}\dot{V}_k \leq & -\frac{\sigma_k}{2}(\lambda_Q - 1)\|\boldsymbol{e}_k\|^2 + \sigma_k\boldsymbol{e}_k^T P\boldsymbol{b}(g_k u_k - g_k u_{dk}) \\ & +\sigma_k\boldsymbol{e}_k^T P\boldsymbol{b} g_d[u_{dk} + \boldsymbol{\eta}^T\boldsymbol{\chi}_k + \sum_{j=1}^{p}(\boldsymbol{z}_j^T\boldsymbol{\varphi}_{j,k}\zeta_{j,k})] \\ & +\frac{\sigma_k}{2}\|\boldsymbol{e}_k\|^2 + \sigma_k\alpha^2(\boldsymbol{x}, \boldsymbol{x}_d, k)(\boldsymbol{e}_k^T P\boldsymbol{b})^2 \\ & +\sigma_k\beta^2(\boldsymbol{x}_k, \boldsymbol{x}_d, t)u_{dk}^2(\boldsymbol{e}_k^T P\boldsymbol{b})^2, \end{aligned} \tag{48}$$

where the representation of λ_Q is the same as that in Section 3. On the basis of (48), we design the controller as

$$u_k = u_{dk} - \frac{\boldsymbol{e}_k^T P\boldsymbol{b}}{g_m}\left(\alpha^2(\boldsymbol{x}_k, \boldsymbol{x}_d, t) + \beta^2(\boldsymbol{x}_k, \boldsymbol{x}_d, t)u_{dk}^2\right), \tag{49}$$

$$u_{dk} = -\boldsymbol{\eta}_k^T\boldsymbol{\chi}_k - \sum_{j=1}^{p}(\boldsymbol{\omega}_{j,k}^T\boldsymbol{\varphi}_{j,k}\zeta_{j,k}), \tag{50}$$

$$\boldsymbol{\eta_k} = \mathrm{sat}_{\underline{\eta},\bar{\eta}}(\boldsymbol{\eta}_{k-1}) + \mu_2\sigma_k\boldsymbol{e}_k^T P\boldsymbol{b}\boldsymbol{\psi}_k, \boldsymbol{\eta}_{-1} = 0, \tag{51}$$

$$\boldsymbol{\omega}_{j,k} = \mathrm{sat}_{\underline{\omega}_j,\bar{\omega}_j}(\boldsymbol{\omega}_{j,k-1}) + \mu_3\sigma_k\boldsymbol{e}_k^T P\boldsymbol{b}\boldsymbol{\varphi}_{j,k}\zeta_{j,k}, \boldsymbol{\omega}_{j,-1} = 0, \tag{52}$$

where the learning gains and control parameters may be set similar to the ones in Section III.

Similar to (22), substituting (49) into (48) leads to

$$\begin{aligned}\dot{V}_k \leq & -\frac{\sigma_k}{2}\ell_Q\|\boldsymbol{e}_k\|^2 + \sigma_k\boldsymbol{e}_k^T P\boldsymbol{b}g\big[\tilde{\boldsymbol{\eta}}_k^T\boldsymbol{\psi}_k \\ & +\sum_{j=1}^{p}(\tilde{\boldsymbol{\omega}}_{j,k}^T\boldsymbol{\varphi}_{j,k}\zeta_{j,k})\big] \end{aligned} \tag{53}$$

where $\tilde{\boldsymbol{\eta}}_k = \boldsymbol{\eta} - \boldsymbol{\eta}_k$ and $\tilde{\boldsymbol{\omega}}_{j,k} = \boldsymbol{\omega}_j - \boldsymbol{\omega}_{j,k}$.

The property of the closed-loop system composed of (42), (49)-(52) may be summarized as follows:

Theorem 2: Consider the nonlinear system (42) satisfying Assumption 1-3 and $\boldsymbol{x}_k(0) = \boldsymbol{x}_k(T)$. The proposed robust iterative learning controller (19)-(21) guarantees the tracking performance and system stability as follows:

t4) $\boldsymbol{e}_k^T(t)P\boldsymbol{e}_k(t) < b_e$ holds during each iteration;

t5) All adjustable control parameters and internal signals are bounded;

t6) $\boldsymbol{e}_k(t) = 0$ may be achieved as the iteration number increases.

The proof of Theorem 2 is similar to that of Theorem 1, which is omitted due to space limitation.

VI. NUMERICAL SIMULATION

Consider a nonlinear uncertain system as follows:

$$\begin{cases}\dot{x}_{1,k} = x_{2,k}, \\ \dot{x}_{2,k} = \vartheta_k\sin(x_{1,k}) + \dfrac{10 - 4.5\sin(t) + 3x_{1,k} + x_{2,k}}{1 + 0.1\sin^2(x_{1,k}x_{2,k})} \\ \qquad + \dfrac{1}{1 + 0.1\cos(0.1\pi t)}u_k,\end{cases} \tag{54}$$

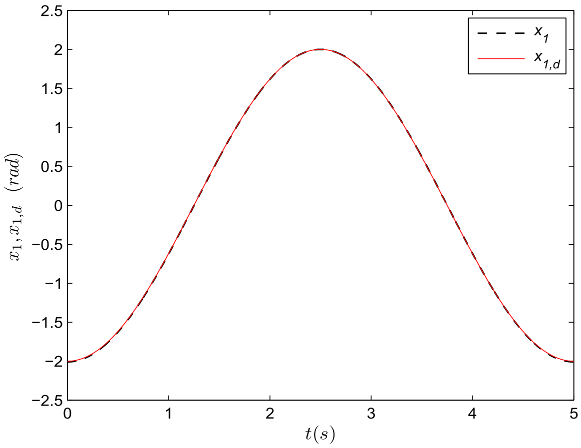

FIGURE 2. **The trajectory of x_1 (Case A).**

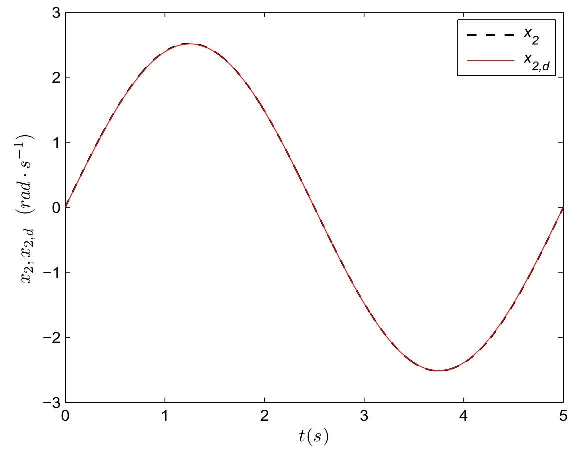

FIGURE 3. **The trajectory of x_2 (Case A).**

where $\frac{10-4.5\sin(t)+3x_{1,k}+x_{2,k}}{1+0.1\sin^2(x_{1,k}x_{2,k})}$ is the nonparametric uncertainty, and $\frac{1}{1+0.1\cos(0.1\pi t)}$ is an unknown iteration-independent but time-varying variable, ϑ_k is an uncertainty generated by HOIM as $\vartheta_k = h_1\vartheta_{k-1} + h_2\vartheta_{k-2}$ with $h_1 = -0.2$, $h_2 = -0.3$, $\vartheta_{-2}(t) = 0.08\cos(\pi t/12)$, $\vartheta_{-1}(t) = 0.8\sin(0.2\pi t)$. The system initial state and reference signal are $\boldsymbol{x}_0(0) = [-2, 0]^T$ and $\boldsymbol{x}_d(t) = [-2\cos(0.25\pi t), 0.5\pi\sin(0.25\pi t)]^T$, respectively.

Case A. The control law(19) and learning laws (20)-(21) are applied in the simulation with $p = 1$, $\mu_1 = 10$, $\mu_2 = 3$, $\mu_3 = 3$, $T = 5$, $b_e = 0.5$,

$$P = \begin{pmatrix} 7.5 & 2.5 \\ 2.5 & 2.5 \end{pmatrix}, Q = \begin{pmatrix} 5 & 0 \\ 0 & 5 \end{pmatrix}. \tag{55}$$

After the ILC system run 100 cycles, the simulation results are shown in Figs. 2-8. Figs. 2-3 show the tracking process during 100th iteration. The profiles of tracking error e_1 and e_2 during 100th iteration are presented in Figs. 4-5. From Figs. 2-5, we can see that satisfactory tracking performance is achieved even in the presence of time-iteration-varying parametric uncertainties and nonparametric uncertainties. The

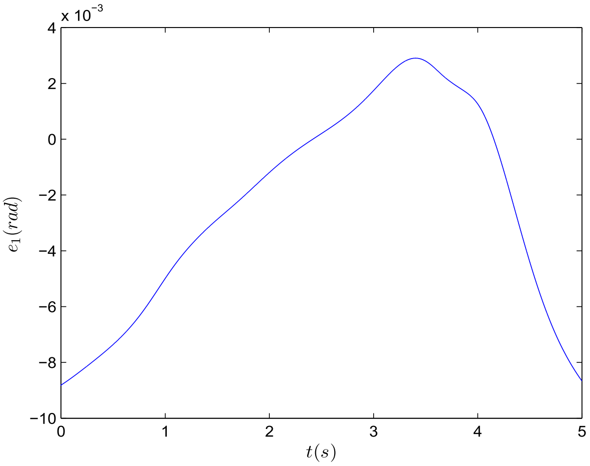

FIGURE 4. The tracking error e_1 (Case A).

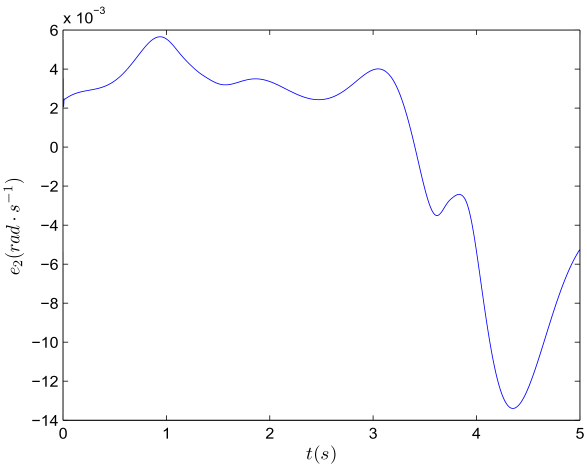

FIGURE 5. The tracking error e_2 (Case A).

convergence history of closed-loop ILC system is provided in Fig. 6, where $J_k := \max_{t\in[0,T]}(\boldsymbol{e}_k^T P \boldsymbol{e}_k)$. From Fig. 6, it can be seen that the excellent system convergence is obtained and the constraint requirement $J_k < b_e$ is met during each iteration. The control signal is plotted in Fig. 7, which shows the continuity and boundedness of the control action.

Case B. A constraint-free adaptive ILC is adopted for comparison as follows:

$$u_k = -\mu_1 \boldsymbol{e}_k^T P \boldsymbol{b} - \boldsymbol{\varpi}_k^T \boldsymbol{\psi}_k - \sum_{j=1}^{p} (\boldsymbol{z}_{j,k}^T \boldsymbol{\varphi}_{j,k} \zeta_{j,k}), \quad (56)$$

$$\boldsymbol{\varpi_k} = \boldsymbol{\varpi}_{k-1} + \mu_2 \boldsymbol{e}_k^T P \boldsymbol{b} \boldsymbol{\psi}_k, \boldsymbol{\varpi}_{-1} = 0, \quad (57)$$

$$\boldsymbol{z}_{j,k} = \boldsymbol{z}_{j,k-1} + \mu_3 \boldsymbol{e}_k^T P \boldsymbol{b} \boldsymbol{\varphi}_{j,k} \zeta_{j,k}, \boldsymbol{z}_{j,-1} = 0, \quad (58)$$

in which the control parameters, learning gains and initial states are set as exactly the same as that in Case A, respectively. Figs. 8-9 show the state tracking trajectories during the 100th iteration. The profiles of corresponding tracking error are given in Figs. 10-11. From Figs. 8-11, it can be seen that accurate trajectory tracking may be obtained as the

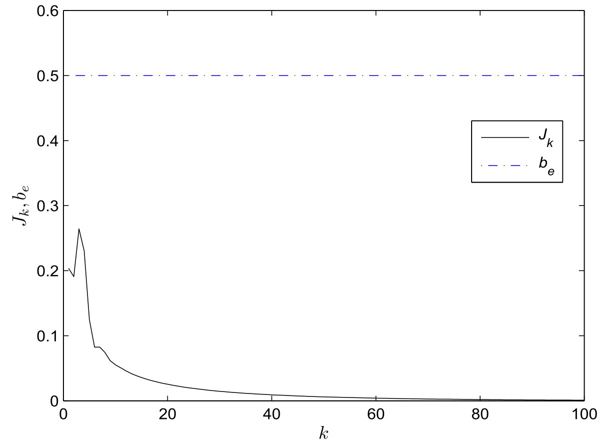

FIGURE 6. Maximum of $|\boldsymbol{e}_k^T P \boldsymbol{e}_k|$ in iteration domain(Case A).

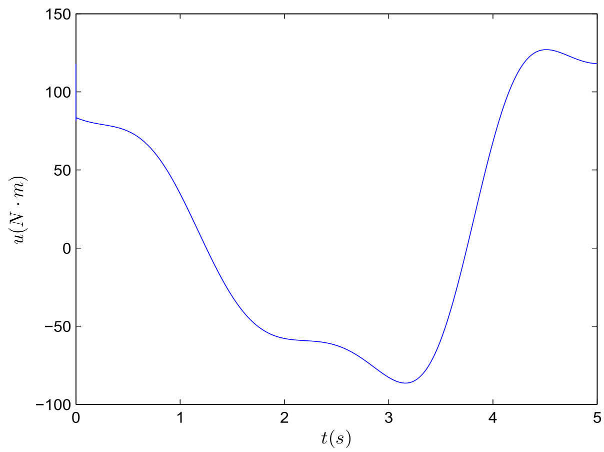

FIGURE 7. Control input(Case A).

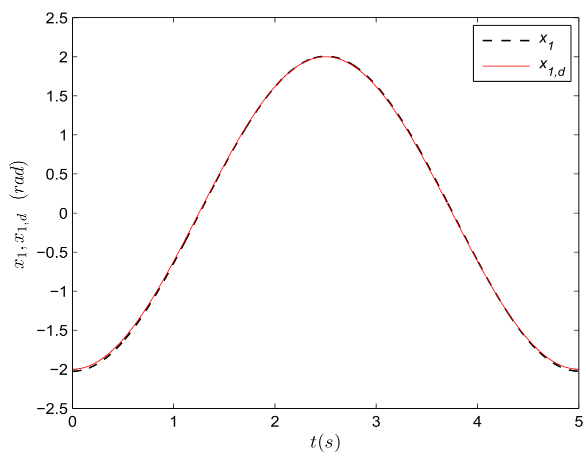

FIGURE 8. The trajectory of x_1 (Case B).

iteration number increases. The convergence history of the constraint-free adaptive ILC is illustrated in Fig. 12. The definition of J_k in Fig. 12 is the same as that in Fig. 6. Compared with Fig. 6, $J_k < b_e$ does not hold in the constraint-free

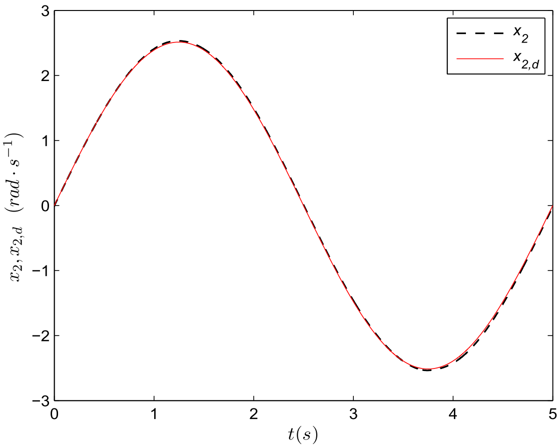

FIGURE 9. The trajectory of x_2 (Case B).

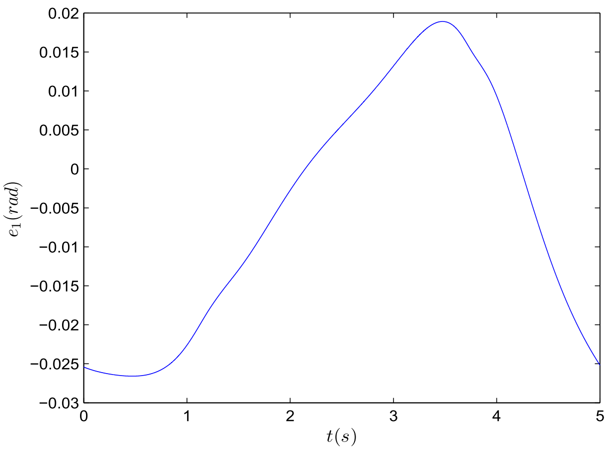

FIGURE 10. The tracking error e_1 (Case B).

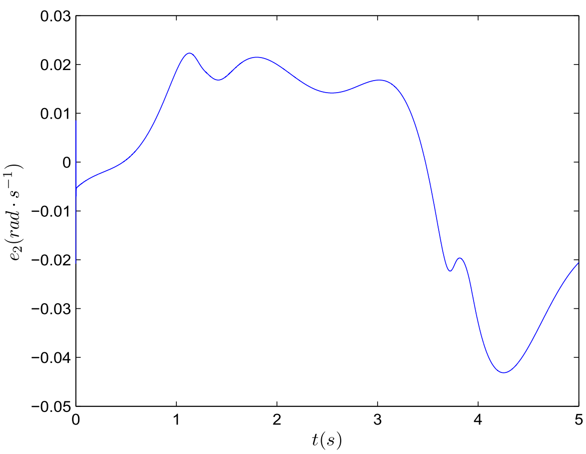

FIGURE 11. The tracking error e_2 (Case B).

ILC system, and the system-constraint ILC system converges faster than the constraint-free ILC system.

Case C. To evaluate the robustness of the ILC algorithm against random parametric uncertainties and random external disturbances, we implement the ILC law (19) and adaptive

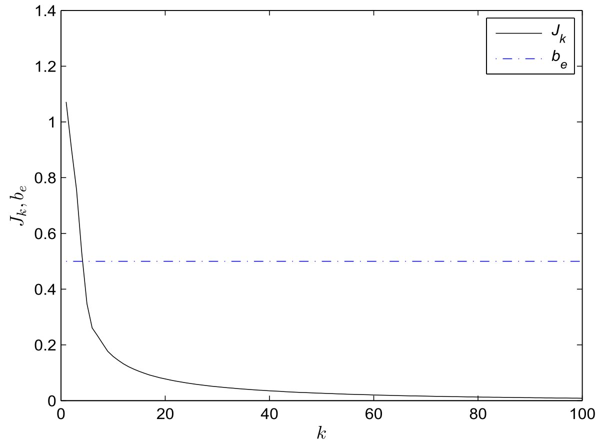

FIGURE 12. Maximum of $|\mathbf{e}_k^T P \mathbf{e}_k|$ in iteration domain(Case B).

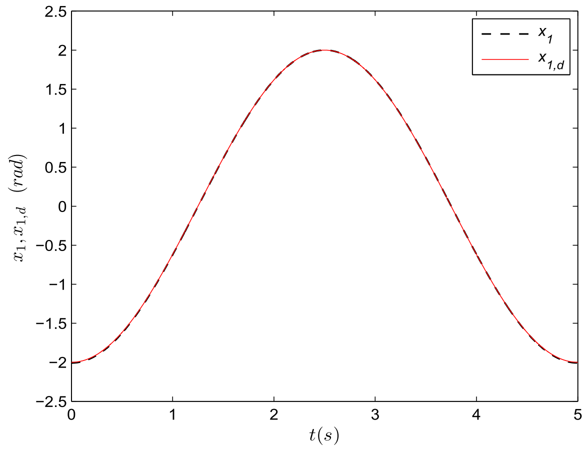

FIGURE 13. The trajectory of x_1 (Case C).

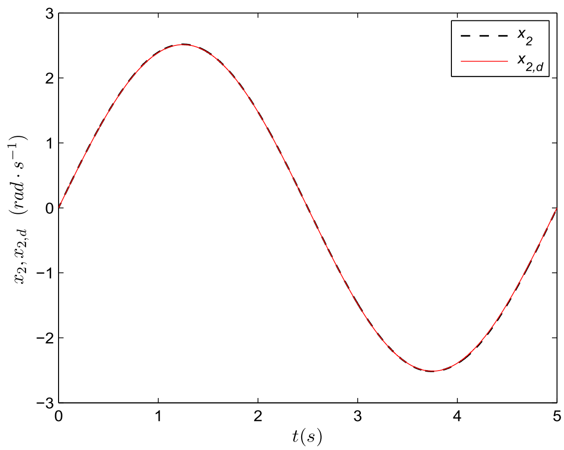

FIGURE 14. The trajectory of x_2 (Case C).

learning laws (20)-(21) to the system as follows:

$$\begin{cases} \dot{x}_{1,k} = x_{2,k}, \\ \dot{x}_{2,k} = (\vartheta_k + 0.5\mathrm{rand}_1(t))\sin(x_{1,k}) + 2\mathrm{rand}_2(t) \\ \qquad + \dfrac{10 - 4.5\sin(t) + 3x_{1,k} + x_{2,k}}{1 + 0.1\sin^2(x_{1,k}x_{2,k})} \\ \qquad + \dfrac{1}{1 + 0.1\cos(0.1\pi t)} u_k, \end{cases} \tag{59}$$

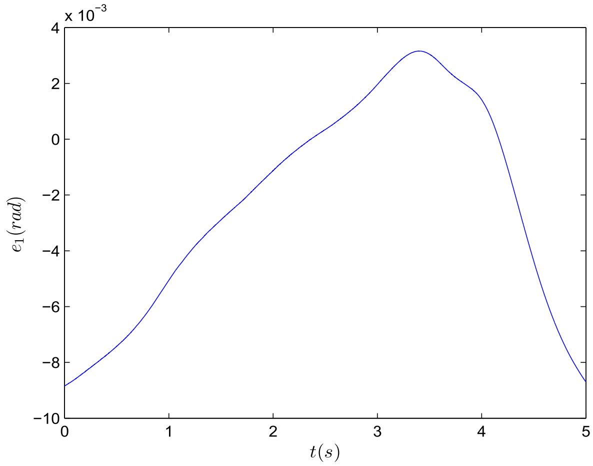

FIGURE 15. The tracking error e_1 (Case C).

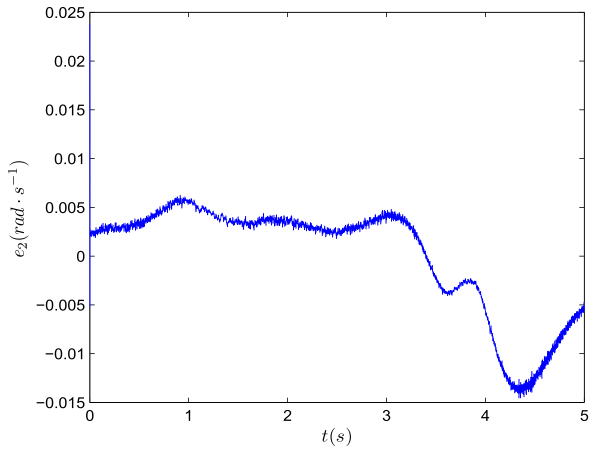

FIGURE 16. The tracking error e_2 (Case C).

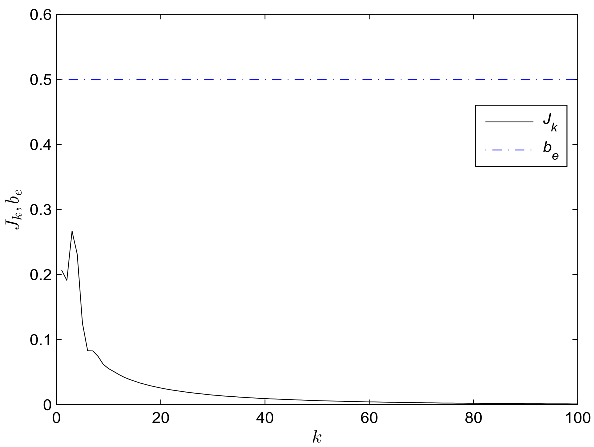

FIGURE 17. Maximum of $|e_k^T P e_k|$ in iteration domain(Case C).

where $\text{rand}_1(\cdot)$ and $\text{rand}_2(\cdot)$ represent two random numbers between 0 and 1, acting as additional random parametric uncertainties and additional random external disturbances. Except for $\text{rand}_1(\cdot)$ and $\text{rand}_2(\cdot)$, all other symbols in (59) have the same definitions as the ones in (54). The state tracking trajectories in this case during 100 iteration are shown in Figs. 13-14. The profiles of tracking error are shown in Figs. 15-16. From Figs. 13-16, we can see that better tracking performance has been obtained even if there exist additional random parametric uncertainties and additional random external disturbances in the system.

The above simulation results verify the effectiveness of theoretical analysis in this work.

VII. CONCLUSION

In this paper, a barrier adaptive ILC scheme is developed to solve the tracking problem for a class of nonlinear systems with both nonparametric uncertainties and time-iteration-varying parametric uncertainties. Robust learning method is used to compensate for the nonparametric uncertainties. The time-iteration-varying parametric uncertainties generated by HOIM are estimated by using difference learning method. A barrier Lyapunov function is adopted for controller design to constrain the error quadratic form during each iteration, with alignment condition used to overcome the initial position problem of ILC. Excellent tracking performance may be obtained as the iteration number increases. In the future, the developed barrier adaptive ILC scheme can be extended to the multi-input and multi-output nonlinear system with both nonparametric uncertainties and time-iteration-varying parametric uncertainties generated by HOIM.

REFERENCES

[1] J.-X. Xu and Y. Tan, "A composite energy function-based learning control approach for nonlinear systems with time-varying parametric uncertainties," *IEEE Trans. Autom. Control*, vol. 47, no. 11, pp. 1940–1945, Nov. 2002.

[2] R. Chi, B. Huang, Z. Hou, and S. Jin, "Data-driven high-order terminal iterative learning control with a faster convergence speed," *Int. J. Robust Nonlinear Control*, vol. 28, no. 1, pp. 103–119, Jan. 2018.

[3] L. Wu, Q. Yan, and J. Cai, "Neural network-based adaptive learning control for robot manipulators with arbitrary initial errors," *IEEE Access*, vol. 7, pp. 180194–180204, 2019.

[4] J. Liu, X. Ruan, and Y. Zheng, "Iterative learning control for discrete-time systems with full learnability," *IEEE Trans. Neural Netw. Learn. Syst.*, vol. 33, no. 2, pp. 629–643, Feb. 2022.

[5] D. Huang, J.-X. Xu, S. Yang, and X. Jun, "Observer based repetitive learning control for a class of nonlinear systems with non-parametric uncertainties," *Int. J. Robust Nonlinear Control*, vol. 25, no. 8, pp. 1214–1229, 2015.

[6] Y. Yu, J. Wan, and H. Bi, "Suboptimal learning control for nonlinearly parametric time-delay systems under alignment condition," *IEEE Access*, vol. 6, pp. 2922–2929, 2018.

[7] C.-J. Chien and A. Tayebi, "Further results on adaptive iterative learning control of robot manipulators," *Automatica*, vol. 44, no. 3, pp. 830–837, Mar. 2008.

[8] Z. Hou, J. Yan, J.-X. Xu, and Z. Li, "Modified iterative-learning-control-based ramp metering strategies for freeway traffic control with iteration-dependent factors," *IEEE Trans. Intell. Transp. Syst.*, vol. 13, no. 2, pp. 606–618, Jun. 2012.

[9] X. Bu, Q. Yu, Z. Hou, and W. Qian, "Model free adaptive iterative learning consensus tracking control for a class of nonlinear multiagent systems," *IEEE Trans. Syst., Man, Cybern., Syst.*, vol. 49, no. 4, pp. 677–686, Apr. 2019.

[10] X. Dai and X. Zhou, "Mixed PD-type iterative learning control algorithm for a class of parabolic singular distributed parameter systems," *IEEE Access*, vol. 9, pp. 12180–12190, 2021.

[11] M. J. Er and J. Xu, "Iterative learning control for systems with both parametric and non-parametric uncertainties," in *Proc. 8th Control, Autom., Robot. Vis. Conf.*, vol. 1, Dec. 2004, pp. 30–35.

[12] C. Yin, J.-X. Xu, and Z. Hou, "A high-order internal model based iterative learning control scheme for nonlinear systems with time-iteration-varying parameters," *IEEE Trans. Autom. Control*, vol. 55, no. 11, pp. 2665–2670, Nov. 2010.

[13] M. Yu, W. Zhou, and B. Liu, "On iterative learning control for MIMO nonlinear systems in the presence of time-iteration-varying parameters," *Nonlinear Dyn.*, vol. 89, no. 4, pp. 2561–2571, 2017.
[14] K. Wan and X.-D. Li, "High-order internal model-based iterative learning control for 2-D linear FMMI systems with iteration-varying trajectory tracking," *IEEE Trans. Syst., Man, Cybern., Syst.*, vol. 51, no. 3, pp. 1462–1472, Mar. 2021.
[15] D. Q. Mayne, J. B. Rawlings, C. V. Rao, and P. O. M. Scokaert, "Constrained model predictive control: Stability and optimality," *Automatica*, vol. 36, no. 6, pp. 789–814, 2000.
[16] K. Kogiso and K. Hirata, "Reference governor for constrained systems with time-varying references," in *Proc. IEEE Int. Conf. Multisensor Fusion Integr. Intell. Syst.*, Sep. 2006, pp. 359–364.
[17] X. Jin, Z. Wang, and R. H. S. Kwong, "Convex optimization based iterative learning control for iteration-varying systems under output constraints," in *Proc. 11th IEEE Int. Conf. Control Autom. (ICCA)*, Jun. 2014, pp. 1444–1448.
[18] K. B. Ngo, R. Mahony, and Z.-P. Jiang, "Integrator backstepping using barrier functions for systems with multiple state constraints," in *Proc. 44th IEEE Conf. Decis. Control*, Dec. 2005, pp. 8306–8312.
[19] L. Liu, Y. J. Liu, S. C. Tong, and C. L. P. Chen, "Integral barrier Lyapunov function-based adaptive control for switched nonlinear systems," *Sci. China Inf. Sci.*, vol. 63, no. 3, pp. 1–14, 2020.
[20] T. Yang, N. Sun, and Y. Fang, "Neuroadaptive control for complicated underactuated systems with simultaneous output and velocity constraints exerted on both actuated and unactuated states," *IEEE Trans. Neural Netw. Learn. Syst.*, early access, Oct. 8, 2021, doi: 10.1109/TNNLS.2021.3115960.
[21] X. Jin and J.-X. Xu, "Iterative learning control for output-constrained systems with both parametric and nonparametric uncertainties," *Automatica*, vol. 49, no. 8, pp. 2508–2516, 2013.
[22] J.-X. Xu and X. Jin, "State-constrained iterative learning control for a class of MIMO systems," *IEEE Trans. Autom. Control*, vol. 58, no. 5, pp. 1322–1327, May 2013.
[23] Q. Z. Yan and M. X. Sun, "Error-tracking iterative learning control with state constrained for nonparametric uncertain systems," *Control Theory Appl.*, vol. 32, no. 7, pp. 895–901, Jul. 2015.
[24] Q. Yu, Z. Hou, and R. Chi, "Adaptive iterative learning control for nonlinear uncertain systems with both state and input constraints," *J. Franklin Inst.*, vol. 353, no. 15, pp. 3920–3943, Oct. 2016.
[25] J. Liu, X. Dong, D. Huang, and M. Yu, "Composite energy function-based spatial iterative learning control in motion systems," *IEEE Trans. Control Syst. Technol.*, vol. 26, no. 5, pp. 1834–1841, Sep. 2018.
[26] Z. Li, C. Yin, H. Ji, and Z. Hou, "Constrained spatial adaptive iterative learning control for trajectory tracking of high speed train," *IEEE Trans. Intell. Transp. Syst.*, vol. 23, no. 8, pp. 11720–11728, Aug. 2022, doi: 10.1109/TITS.2021.3106653.
[27] Z. Yang, W. Wang, Y. Zhang, Q. Yan, and J. Cai, "High-order internal model based barrier iterative learning control for time-iteration-varying parametric uncertain systems with arbitrary initial errors," *IEEE Access*, vol. 10, pp. 17619–17628, 2022.
[28] J.-X. Xu and R. Yan, "On initial conditions in iterative learning control," *IEEE Trans. Autom. Control*, vol. 50, no. 9, pp. 1349–1354, Sep. 2005.
[29] C.-J. Chien, C.-T. Hsu, and C.-Y. Yao, "Fuzzy system-based adaptive iterative learning control for nonlinear plants with initial state errors," *IEEE Trans. Fuzzy Syst.*, vol. 12, no. 5, pp. 724–732, Oct. 2004.
[30] X.-D. Li, M.-M. Lv, and J. K. L. Ho, "Adaptive ILC algorithms of nonlinear continuous systems with non-parametric uncertainties for non-repetitive trajectory tracking," *Int. J. Syst. Sci.*, vol. 47, no. 10, pp. 2279–2289, 2016.
[31] Q. Z. Yan and M. X. Sun, "Iterative learning control for nonlinear uncertain systems with arbitrary initial state," *Acta Autom. Sinica*, vol. 42, no. 4, pp. 545–555, Apr. 2016.
[32] J.-X. Xu, X. Jin, and D. Huang, "Composite energy function-based iterative learning control for systems with nonparametric uncertainties," *Int. J. Adapt. Control Signal Process.*, vol. 28, no. 1, pp. 1–13, 2014.
[33] C. E. Boudjedir, M. Bouri, and D. Boukhetala, "Iterative learning control for trajectory tracking of a parallel delta robot," *Automatisierungstechnik*, vol. 67, no. 2, pp. 145–156, Feb. 2019.
[34] T. Yang, N. Sun, and Y. Fang, "Adaptive fuzzy control for a class of MIMO underactuated systems with plant uncertainties and actuator deadzones: Design and experiments," *IEEE Trans. Cybern.*, vol. 52, no. 8, pp. 8213–8226, Aug. 2022, doi: 10.1109/TCYB.2021.3050475.

ZHONGJIE HE (Member, IEEE) received the B.S. degree in automation from Hangzhou Dianzi University, Hangzhou, China, in 2003, and the Ph.D. degree in electrical engineering from Zhejiang University, Hangzhou, in 2009. From 2009 to 2012, he worked as an Electrical Engineer at the Zhejiang Electric Power Planning and Design Institute, State Grid, Hangzhou. Since 2012, he has been working as a Lecturer at the College of Automation, Hangzhou Dianzi University. His current research interests include artificial intelligence, adaptive control, scheduling optimization, and muti-objective programming. He is a member of the Chinese Association of Artificial Intelligence and the Director of the IEEE PES Electric Vehicle Satellite Committee-China.

JIANNING LI received the Ph.D. degree in control science and engineering from Zhejiang University, Hangzhou, China, in 2013. In 2012, he was a Visiting Scholar with the Department of Mechanical Engineering, Dalhousie University, Halifax, NS, Canada. From 2018 to 2019, he was a Visiting Scholar with the Department of Electrical and Computer Engineering, University of California, Riverside, CA, USA. He is currently an Associate Professor with the School of Automation, Hangzhou Dianzi University, Hangzhou. His research interests include fault-tolerant control, robust control, and networked control systems.